

• 临床研究 •

从组织特征筛选 qPCR 阳性标本: 快捷、准确、经济诊断肺结核

沈丽华, 张倩倩, 金晓燕, 胡慧娣, 董燕, 邹珏*

南京医科大学附属脑科医院(南京市胸科医院)病理科, 江苏 南京 210029

[摘要] 目的: HE染色评估组织病理学特征、初筛实时荧光定量PCR(real-time fluorescent quantitative PCR, qPCR)阳性率高的标本, 快捷、准确、经济地诊断肺结核。方法: 回顾性分析189例肺肉芽肿疾病患者的临床资料和CT征象, 采用苏木精-伊红(hematoxylin-eosin, HE)染色对甲醛固定、石蜡包埋(formalin-fixed paraffin-embedded, FFPE)标本初筛后行Ziehl-Neelsen(Z-N)抗酸染色和qPCR检测进一步验证。结果: 189例标本根据CT征象可分为两组: 周围型结节组多表现为肺门纵隔淋巴结肿大(87/149, 58.4%)、分叶征(66/149, 44.3%)和毛刺征(63/149, 42.3%); 中央型占位组主要征象为支气管阻塞(31/40, 77.5%)、肺不张(29/40, 72.5%)。这些征象与肿瘤性病难以区分, 常导致诊断延误。95例确诊肺结核标本的HE染色结果显示: 坏死面积百分比 $\geq 25\%$ ($\chi^2=41.649, P < 0.001$)、肉芽肿最大直径 ≥ 8 mm ($\chi^2=8.071, P=0.004$)与qPCR阳性结果呈正相关。二元Logistic回归分析显示, 肺结核坏死面积百分比和肉芽肿最大直径是qPCR阳性的独立预测因子(OR=1.324, 95%CI: 1.202~1.460, $P < 0.001$; OR=0.265, 95%CI: 0.164~0.429, $P < 0.001$)。在肺结核FFPE标本中, 坏死面积百分比检测qPCR阳性结果的曲线下面积、灵敏度、特异度分别为0.794、78.2%、78.9%, 而肉芽肿最大直径检测qPCR阳性结果的曲线下面积、灵敏度、特异度则分别为0.600、88.5%和43.7%。结论: 外周型结节CT征象表现为肺门及纵隔淋巴结肿大、分叶征和毛刺征时, 更容易引起肺结核等肉芽肿性疾病的延误诊断; 坏死面积和肉芽肿最大直径测量可提高qPCR检测的灵敏度, 通过HE染色初筛选择优质标本进行检测, 可提高结核病诊断的准确性。

[关键词] 肺结核; 定量PCR; 组织病理学特征; 辅助诊断**[中图分类号]** R521**[文献标志码]** A**[文章编号]** 1007-4368(2025)09-1316-10

doi: 10.7655/NYDXBNSN250203

Screening qPCR-positive specimens based on histopathological characteristics: a rapid, accurate, and economical diagnosis of pulmonary tuberculosis

SHEN Lihua, ZHANG Qianqian, JIN Xiaoyan, HU Huidi, DONG Yan, ZOU Jue*

Department of Pathology, the Affiliated Brain Hospital of Nanjing Medical University (Nanjing Chest Hospital), Nanjing 210029, China

[Abstract] **Objective:** To screen specimens with high qPCR positive rates based on hematoxylin and eosin (HE) histopathological characteristics for the rapid, accurate, and economical diagnosis of pulmonary tuberculosis. **Methods:** A retrospective analysis was conducted on the clinical data and CT findings of 189 patients with pulmonary granulomatous disease. Formalin-fixed paraffin-embedded (FFPE) specimens were initially screened by HE staining, followed by Ziehl-Neelsen (Z-N) staining and qPCR assay for further verification. **Results:** Based on CT findings, 189 specimens were divided into two groups: the peripheral nodular group predominantly showed hilar and mediastinal lymphadenopathy (87/149, 58.4%), lobulation sign (66/149, 44.3%), and spiculation sign (63/149, 42.3%); and the central occupancy group mainly exhibited bronchial obstruction (31/40, 77.5%) and atelectasis (29/40, 72.5%). These findings were often indistinguishable from neoplastic lesions, leading to delayed diagnoses. HE staining results from 95 confirmed pulmonary tuberculosis specimens revealed that the percentage of necrotic area $\geq 25\%$ ($\chi^2=41.649, P < 0.001$) and the maximum diameter of granulomas ≥ 8 mm ($\chi^2=8.071, P=0.004$) were correlated with qPCR positivity. Binary logistic regression analysis showed that the percentage of necrotic area and the maximum diameter of granulomas in pulmonary tuberculosis were independent predictors of qPCR positivity (OR=1.324, 95%CI: 1.202~1.460, $P < 0.001$; OR=0.265, 95%CI: 0.164~0.429, $P < 0.001$).

[基金项目] 北京市希思科学肿瘤学研究基金

*通信作者(Corresponding author), E-mail: Zoujue1981@126.com (ORCID: 0000-0002-7749-6812)

In FFPE specimens of pulmonary tuberculosis, the area under the curve, sensitivity, and specificity of the necrotic area percentage for qPCR positive results were 0.794, 78.2% and 78.9%, while for the maximum diameter of granulomas were 0.600, 88.5%, and 43.7%, respectively. **Conclusion:** When CT findings of peripheral nodules show hilar and mediastinal lymphadenopathy, lobulation sign, and spiculation sign, they are more likely to delay diagnosis of granulomatous diseases such as pulmonary tuberculosis. The measurement of necrotic area and the maximum diameter of granulomas can improve the sensitivity of qPCR detection. Preliminary screening with HE staining to select high-quality specimens for testing can enhance the accuracy of tuberculosis diagnosis.

[Key words] pulmonary tuberculosis; quantitative PCR; histopathological features; auxiliary diagnosis

[J Nanjing Med Univ, 2025, 45(09): 1316-1325]

结核病(tuberculosis, TB)是结核分枝杆菌(*Mycobacterium tuberculosis*, MTB)引起的一种空气传播疾病,通常会影晌肺部,导致严重的咳嗽、发烧和胸痛^[1]。尽管在疫苗接种、治疗和诊断方面取得了进展,但TB仍然是全球健康面临的巨大挑战^[2]。早期诊断对于有效切断疾病传播和提高治疗效果至关重要^[3-5]。

包括TB在内的肺肉芽肿类疾病的早期筛查主要依赖于胸部影像学检查,但部分病变并不典型,表现出多样性,与恶性肿瘤难以鉴别。因此,支气管内超声引导下经支气管针吸活检(endobronchial ultrasound-guided transbronchial needle aspiration, EBUS-TBNA)、经皮肺穿刺活检(percutaneous needle lung biopsy, PNLB)或手术切除肺肉芽肿类标本在肺结核的诊断中具有重要意义。这些标本提供了详细的组织学信息,有助于识别结核特征性病变^[6]。

对石蜡包埋(formalin-fixed paraffin-embedded, FFPE)标本进行抗酸染色是TB病理诊断的传统金标准之一^[7-8]。该方法通过在显微镜下观察石蜡切片中抗酸杆菌的存在来确诊结核感染。它对样本质量要求较高,如果样本中细菌数量较少或细菌分布不均,可能会导致结果不可靠^[9]。显微镜下观察染色阳性标本,很难区分MTB和非结核分枝杆菌(nontuberculous mycobacteria, NTM),因为这两种分枝杆菌都耐酸且形态相似^[10]。因此,抗酸染色在肺组织FFPE标本上的检测灵敏度和特异度非常低,其结果的判定也取决于技术人员的主观判断^[11-12]。因此,在典型的TB诊断流程中,虽然抗酸染色通常作为初筛手段,但需要后续的分于检测技术复核以明确最终的诊断结果。

随着分子检测技术的发展,实时荧光定量PCR(real-time fluorescent quantitative PCR, qPCR)被引入TB检测中^[13]。针对仅存在于MTB中的插入元件IS6110靶基因的qPCR检测具有特异性高、检测周

期短、能够区分混合感染、不需要生物安全3级设施、相对容易自动化操作等优点^[14-16]。但在实际操作过程中,研究人员也发现并不适合所有类型的标本^[17-18],选择不恰当的蜡块检测将导致最终结果不可靠,造成诊断延迟,且由于其成本相对较高,增加了TB患者的经济负担。

HE染色是组织病理学中最常用的方法,具有典型结核特征的标本可以通过常规HE染色进行可靠的TB推定诊断,观察组织切片,可以识别出TB的一些特征性病理改变,包括肉芽肿形成、干酪样坏死、朗汉斯巨细胞、纤维化等^[19]。由于HE染色主要用于显示组织结构和炎症反应,而不是直接检测MTB,在TB初始筛查中具有很高的敏感性^[20]。且操作简单、成本低廉,适用于大规模筛查和初步诊断,在资源有限的环境中尤为实用,能够快速提供初步诊断信息,从而决定是否需要进行进一步检测。

基于上述背景,本研究选择189例因CT征象不典型、未取得呼吸道分泌物标本或分泌物标本MTB检测结果为阴性而行EBUS-TBNA、PNLB或外科手术的肉芽肿疾病患者,采用HE染色对其进行初始筛查,筛选出149例具有TB典型特征的标本行Ziehl-Neelsen(Z-N)抗酸染色和qPCR检测;同时,通过HE染色观察TB标本的特征性病理改变,分析这些病理特征与qPCR结果之间的相关性。旨在通过HE染色筛选出具有典型qPCR阳性特征的标本,直接进行qPCR检测,从而简化诊断步骤,降低成本,提高诊断的准确性和效率,并提出一种快捷、准确、经济的TB诊断流程。

1 对象和方法

1.1 对象

对南京医科大学附属脑科医院(南京市胸科医院)2020年1月—2022年12月189例经EBUS-TBNA、PNLB或外科手术的肉芽肿疾病患者的临床和影像

学资料进行回顾性分析,从病理科获得组织蜡块用于本研究。纳入标准:胸部CT提示肺部异常,但缺乏典型TB表现(TB的典型胸部CT表现包括斑块、空洞影、结节、树芽征、纤维条纹、继发性支气管扩张、多发钙化、空洞形成,而继发性支气管扩张、多发性钙化、空洞形成等好发于上叶尖段或后段及下叶背段,多种形态的病变共存)^[21],与肿瘤不能鉴别者;临床表现无典型的TB症状如咳嗽、咳痰、咯血及发热等;缺乏痰、肺泡灌洗液等呼吸道分泌物MTB检测或检测结果为阴性。组织标本来源于EBUS-TBNA、PNLB或外科手术。本研究经南京医科大学附属脑科医院(南京胸科医院)伦理委员会批准(2024-KY026-01),符合赫尔辛基宣言及其后来的修正案。

1.2 方法

1.2.1 Z-N抗酸染色

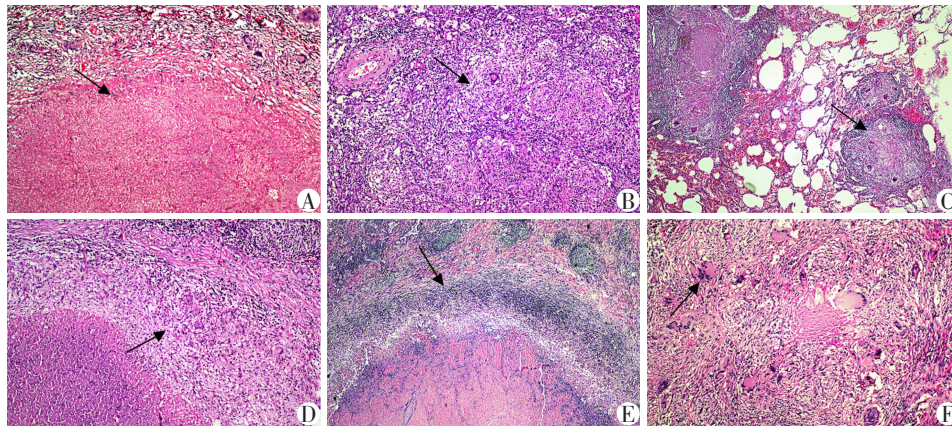
石蜡包埋组织切片厚度为4 μm ,在37 $^{\circ}\text{C}$ 下贴片、干燥、烘烤,二甲苯脱蜡2次,每次5 min,去离子水冲洗2 min;37 $^{\circ}\text{C}$ 石炭酸红染色液染色30 min,染

色过程中观察染色液的液位;去离子水冲洗2 min;5%盐酸乙醇分化液分化2~3 s,直至切片无色;去离子水冲洗2 min;美蓝溶液重新染色20 s;去离子水冲洗2 min;常规脱水、干燥、封片。阳性染色结果为MTB呈鲜红色,细长状,微弯曲的杆状或念珠菌样堆状或散在分布,红细胞呈粉红色,细胞核和背景呈浅蓝色。

1.2.2 HE染色初筛和评估

两名病理医生检查HE染色切片,评估7个组织病理学参数:干酪样坏死面积百分比(坏死的脱细胞粉红色区域伴有核团状碎片 $\geq 25\%$ 或 $< 25\%$),每切片肉芽肿的数目和大小(最大直径 $\geq 8\text{ mm}$ 或 $< 8\text{ mm}$),融合性肉芽肿(多个大小较一致的肉芽肿结节呈融合性生长),离散性肉芽肿(边界分明,大部分上皮样组织细胞与肉芽肿形状一致),上皮样组织细胞带(上皮样组织细胞聚集在坏死的外层),分别评估并记录肉芽肿周围淋巴细胞聚集和朗汉斯巨细胞(图1)。

使用Image J软件对HE染色后的切片进行分



A: Thorough caseous necrosis, acellular pink areas of necrosis with karyorrhectic debris. B: Confluent granulomas, merging of the adjacent boundaries of granulomas. C: Discrete granuloma with well-defined boundaries. D: Lightly stained epithelioid cells aggregate in the outer layer of necrosis. E: Layers of lymphocytes around the granulomas. F: Langerhans' giant cells.

图1 qPCR阳性病例的病理组织学特征(HE, $\times 200$)

Figure 1 Histopathological parameters of qPCR positive samples(HE, $\times 200$)

析。将图像导入软件,利用软件测量工具,在适当放大倍数下,选取需要测量的染色区域进行自动计算并记录相关数据。对于复杂的组织结构,两位资深病理医生采用手动勾勒边界的方式进行精准测量,以确保获取准确的染色面积数据。

1.2.3 qPCR检测

按照说明书,用E.Z.N.A. FFPE DNA试剂盒(Omega Bio-Tek公司,美国)提取DNA,然后用MTB复合核酸检测试剂盒(厦门致善公司)检测。本

试剂盒采用qPCR法检测MTB特异性插入序列IS6110基因。将两端标记有荧光发光基因和淬灭基因的寡核苷酸探针加入PCR系统中,在PCR过程中扩增出与探针序列互补的产物,同时实时监测荧光值变化,通过有无扩增信号来判断是否存在MTB。PCR反应条件为:37 $^{\circ}\text{C}$ 10 min;95 $^{\circ}\text{C}$ 10 min;95 $^{\circ}\text{C}$ 10 s,71 $^{\circ}\text{C}$ 15 s(每个循环下降1度),78 $^{\circ}\text{C}$ 15 s,10个循环;95 $^{\circ}\text{C}$ 15 s,61 $^{\circ}\text{C}$ 15 s(收集荧光信号),78 $^{\circ}\text{C}$ 15 s,45次循环。

结果判断: 若检测样本的靶基因在用于检测MTB基因的6-羧基荧光素(6-carboxyfluorescein, FAM)通道中有明显的S型扩增曲线, 所得Ct值 ≤ 25 , 则判定为阳性, 若Ct值 > 25 或无扩增信号, 则判定为阴性。

1.3 统计学方法

采用SPSS25.0软件进行统计学分析, 进行卡方检验(校准卡方检验)和二元Logistic回归分析, 受试者工作特征(receiver operating characteristic, ROC)曲线分析曲线下面积(area under curve, AUC)、诊断灵敏度和特异度。采用四格表进行Kappa同一性检验, 计算灵敏度、特异度、阳性预测值(positive predictive value, PPV)、阴性预测值(negative predictive value, NPV)。Kappa值 ≤ 0.20 、 $> 0.20 \sim 0.40$ 、 $> 0.40 \sim 0.60$ 、 $> 0.60 \sim 0.80$ 和 > 0.80 分别被认为是轻微、一般、中等、实质性一致和几乎完全一致。 $P < 0.05$ 为差异有统计学意义。

2 结果

2.1 临床特征

在研究期间, 189例患有肺肉芽肿疾病的患者接受了支气管镜检查或外科手术, 年龄24~80岁, 中位年龄为61岁。男119例(63.0%, 119/189), 女70例

(37.0%, 70/189), 男性患者比例高于女性。

观察并记录了189例患者的胸部CT表现, 根据胸部CT表现分为两个亚组, 即周围型结节组($n=149$)和中央型占位组($n=40$)。94/189例(49.7%)的病灶位于TB的典型发病部位, 73/189(38.6%)的患者病灶出现在多个节段, 符合TB特征, 但TB常见的CT表现如空洞(7/189, 3.7%)、局限性支气管扩张(10/189, 5.3%)、卫星灶(0/189, 0%)、树芽征(0/189, 0%)却很少见。而肺门纵隔淋巴结肿大的比例很高(111/189, 58.7%)。

两种不同亚组之间, 周围型结节组多表现为肺门纵隔淋巴结肿大(87/149, 58.4%), 其次为分叶征(66/149, 44.3%)和毛刺征(63/149, 42.3%), 部分患者可伴有胸膜凹陷征(41/149, 27.5%)和胸腔积液(35/149, 23.5%); 少数病例有肺不张(22/149, 14.8%)、支气管阻塞(16/149, 10.7%)、局限性支气管扩张(10/149, 6.7%)及血管束征(4/149, 2.7%); 中央型占位组的表现主要为支气管阻塞(31/40, 77.5%)、肺不张(29/40, 72.5%), 部分患者有肺门纵隔淋巴结肿大(24/40, 60.0%), 少数患者有毛刺征(4/40, 10.0%)及分叶征(3/40, 7.5%)。这些特征往往让医生忽视了某些TB征象, 如病变位于TB好发区、多节段分布等, 从而优先考虑肿瘤性疾病(表1)。

表1 患者胸部CT特征

Table 1 Chest CT features of patients

Chest CT features	Peripheral nodules group ($n=149$)	Central occupancy group ($n=40$)	Total ($n=189$)
Main lesion size(mm, $\bar{x} \pm s$)	22.5 \pm 2.5	21.7 \pm 9.5	21.9 \pm 8.3
Main lesion was located in the predilection sites*[$n(\%)$]	73(49.0)	21(52.5)	94(49.7)
Multi-segmental lesion[$n(\%)$]	47(31.5)	26(65.0)	73(38.6)
Cavity[$n(\%)$]	5(3.4)	2(5.0)	7(3.7)
Lobulation sign[$n(\%)$]	66(44.3)	3(7.5)	69(36.5)
Spiculation sign[$n(\%)$]	63(42.3)	4(10.0)	67(35.4)
Vessel convergence sign[$n(\%)$]	4(2.7)	0(0)	4(2.1)
Pleural indentation[$n(\%)$]	41(27.5)	1(2.5)	42(22.2)
Hilar and mediastinal lymphadenopathy[$n(\%)$]	87(58.4)	24(60.0)	111(58.7)
Bronchial obstruction[$n(\%)$]	16(10.7)	31(77.5)	47(24.9)
Localized bronchiectasis[$n(\%)$]	10(6.7)	0(0)	10(5.3)
Atelectasis[$n(\%)$]	22(14.8)	29(72.5)	51(27.0)
Air bronchogram sign[$n(\%)$]	24(16.1)	0(0)	24(12.7)
Pleural effusion[$n(\%)$]	35(23.5)	20(50.0)	55(29.1)
Satellite nodules[$n(\%)$]	0(0)	0(0)	0(0)
Tree-bud sign[$n(\%)$]	0(0)	0(0)	0(0)
Fibrous stripes[$n(\%)$]	29(19.5)	8(20.0)	37(19.6)
Calcification[$n(\%)$]	0(0)	9(22.5)	9(4.8)

*: Predilection sites were apical-posterior segment of the upper lobe and the dorsal segment of the lower lobe.

2.2 HE染色初筛结果

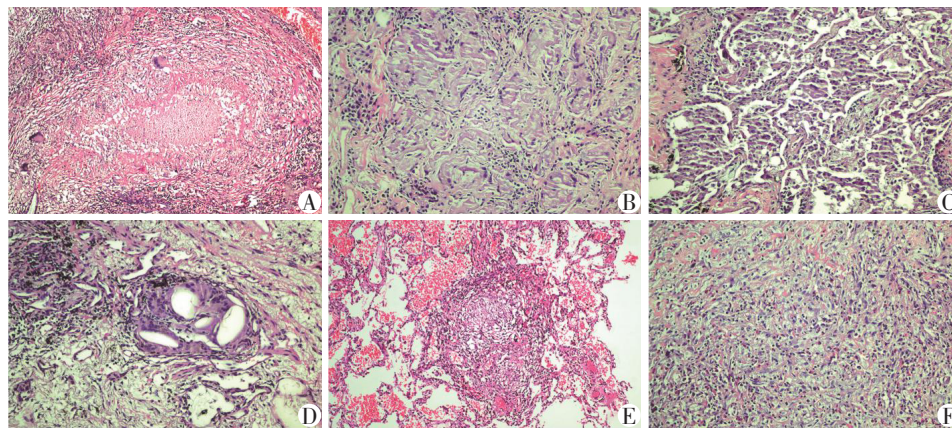
189例肺肉芽肿疾病患者中,周围型结节组以外科手术为主128例(128/149, 85.9%),其次为PNLB(21/149, 14.1%);中央型占位组以EBUS-TBNA为主(31/40, 77.5%),少数为PNLB(9/40, 22.5%)。

采用HE染色进行组织病理学初筛,149例(78.8%, 149/189)具备典型的结核性标本特征,包括干酪样坏死的肉芽肿,或存在上皮样细胞/多核巨细胞,判定为疑似结核感染,待进一步验证。其余40例分别为非结核感染性肉芽肿:异物肉芽肿2例(5.0%, 2/40),反应性多核巨细胞增生11例(27.5%, 11/40),胆固醇结晶形成5例(12.5%, 5/40),其他急性慢性非特异性炎22例(55.0%, 22/40)(图2)。

2.3 Z-N抗酸染色与qPCR法检测MTB与临床诊断的比较

表2总结了149例通过HE初筛、疑似为TB标本,经Z-N抗酸染色和qPCR检测的结果。根据病理检测结果,Z-N抗酸染色和qPCR均为阳性结果确诊54例;在这两项检测之一为阴性的患者中,临床医生结合患者的影像学特征、临床表现、既往经验判断以及患者对诊断性抗结核治疗反应良好的原则确诊TB 41例。临床最终确诊95例TB阳性、54例TB阴性。

以临床诊断作为参考标准,从诊断效率来看,qPCR检测的灵敏度、特异度、PPV、NPV分别为80.0%、96.3%、97.4%和73.2%,高于Z-N抗酸染色(分别为56.8%, 42.6%, 63.5%和35.9%),各组数据



A: Typical granuloma. B: Foreign body granuloma reaction. C: Multinucleated giant cell reaction. D: Cholesterol crystallization formation. E: Non-specific infectious granuloma. F: Non-specific acute and chronic infection.

图2 189例肺肉芽肿病例经HE染色初筛情况(HE, ×100)

Figure 2 Initial screening results of HE staining for 189 cases of pulmonary granulomatous diseases(HE, ×100)

之间的差异均有统计学意义($P < 0.001$)。qPCR检测与临床最终确诊结果的一致性(kappa=0.71)较高。

2.4 qPCR阳性组的组织病理学特征

基于HE染色的qPCR阳性和阴性组的组织病

理学特征(表3),发现坏死面积百分比 $\geq 25\%$ ($\chi^2 = 41.649, P < 0.001$)、肉芽肿最大直径 $\geq 8\text{ mm}$ ($\chi^2 = 8.071, P = 0.004$)与qPCR阳性的相关性更高,差异有统计学意义(表3,图3)。其他病理特征如融合性肉

表2 与临床诊断相比,Z-N抗酸染色和qPCR检测的灵敏度、特异度、PPV、NPV和一致性

Table 2 Sensitivity, specificity, PPV, NPV, and agreement of Z-N staining and qPCR detection compared with clinical diagnosis

Methods		Clinical diagnosis		Sensitivity(%)	Specificity(%)	PPV(%)	NPV(%)	Kappa
		+(n=95)	-(n=54)					
Z-N	+	54	31	56.8	42.6	63.5	35.9	-0.05
	-	41	23					
qPCR	+	76	2	80.0	96.3	97.4	73.2	0.71
	-	19	52					

Z-N: Ziehl-Neelsen staining; qPCR: real-time fluorescent quantitative PCR; +: positive result; -: negative result; PPV: positive predictive value; NPV: negative predictive value.

芽肿、离散性肉芽肿、上皮样组织细胞带、淋巴细胞聚集和朗汉斯巨细胞对qPCR结果无显著影响。因此,测量和计算坏死面积百分比和肉芽肿最大直径有助于预测qPCR结果。

表3 qPCR阳性组与阴性组的组织病理特征比较
Table 3 Comparison of histopathologic parameters between qPCR positive and negative groups (n)

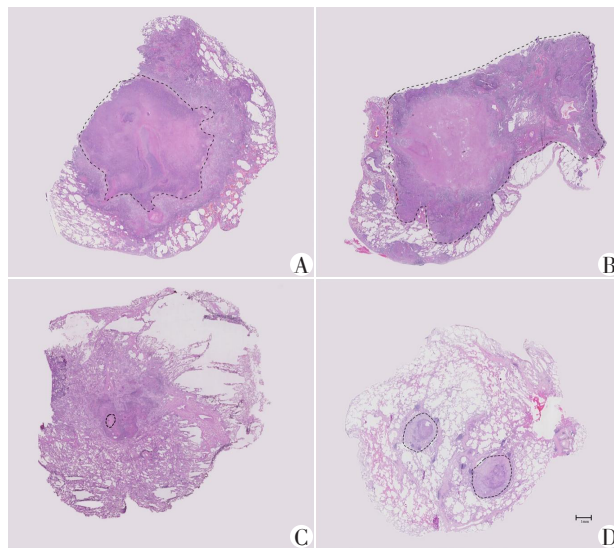
Histopathologic parameter	qPCR+ (n=78)	qPCR- (n=71)	χ^2	P
Necrotic area percentage			41.649	<0.001
$\geq 25\%$	62	19		
<25%	16	52		
Size of granulomas			8.071	0.004
The maximum diameter ≥ 8 mm	50	29		
The maximum diameter <8 mm	28	42		
Confluent granulomas			0.052	0.820
qPCR+	73	68		
qPCR-	5	3		
Discrete granulomas			0.072	0.788
qPCR+	50	44		
qPCR-	28	27		
Bands of epithelioid histiocytes			0.673	0.412
qPCR+	50	41		
qPCR-	28	30		
Lymphoid aggregates			1.224	0.269
qPCR+	65	54		
qPCR-	13	17		
Langerhans' giant cells			1.224	0.265
qPCR+	53	42		
qPCR-	25	29		

2.5 组织病理学特征与qPCR诊断敏感性的相关性分析

为进一步证实组织病理特征对qPCR结果的影响,进行了相关分析(图4)。坏死面积百分比和肉芽肿最大直径与qPCR阳性结果有显著相关性(OR=1.324, 95%CI: 1.202~1.460; OR=0.265, 95%CI: 0.164~0.429)。Hosmer-Lemeshow 检验结果吻合较好($\chi^2=10.227, P>0.05$)。这些结果表明,这两种组织病理学特征可能对TB诊断有辅助作用。

2.6 坏死面积百分比及肉芽肿最大直径的检测效率分析

如图5所示,坏死面积百分比的AUC为0.794,灵敏度为78.2%,特异度为78.9%,95%CI为0.717~0.871 ($P < 0.001$)。肉芽肿最大直径的AUC为



A: The percentage of necrotic area $\geq 25\%$. B: The percentage of necrotic area <25%. C: The maximum diameter of granulomas ≥ 8 mm. D: The maximum diameter of granulomas <8 mm.

图3 测量并计算每张HE切片中坏死面积百分比以及肉芽肿最大直径

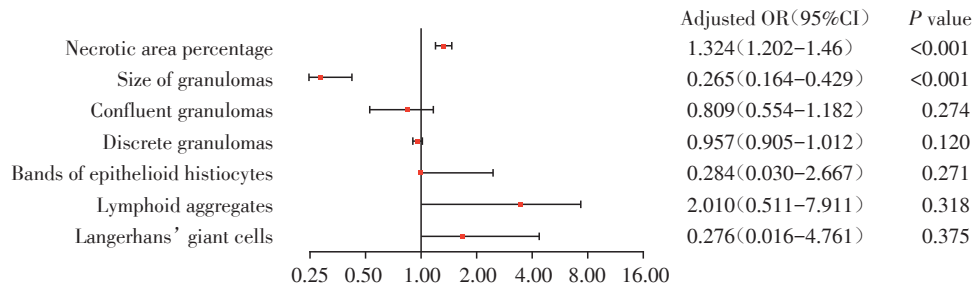
Figure 3 Measurement and calculation of necrotic area percentage and the maximum diameter of granulomas on each HE piece

0.600,灵敏度为88.5%,特异度为43.7%,95%CI为0.505~0.694 ($P=0.036$)。以上结果表明,坏死面积百分比和肉芽肿最大直径对qPCR阳性具有较高的诊断效能,可作为qPCR检测TB的辅助诊断指标。

3 讨论

不典型的CT特征常引起肺部肉芽肿性感染的延误诊断^[22]。招募的189例经EBUS-TBNA、PNLB或外科手术的肉芽肿疾病患者,因放射学表现呈现出分叶征、毛刺征、肺门及纵隔淋巴结肿大等提示恶性肿瘤的特征,而感染相关的其他显著征象如条索影、卫星灶、树芽征、钙化等并不明确,而被首先怀疑为肺癌,诊断过程中缺少呼吸道分泌物的MTB检测结果或检测结果为阴性;其中,40例为中央型肿块,事先完成了支气管镜检查 and PNLB,另外149例患者中,21例行PNLB,其余接受了外科手术治疗。

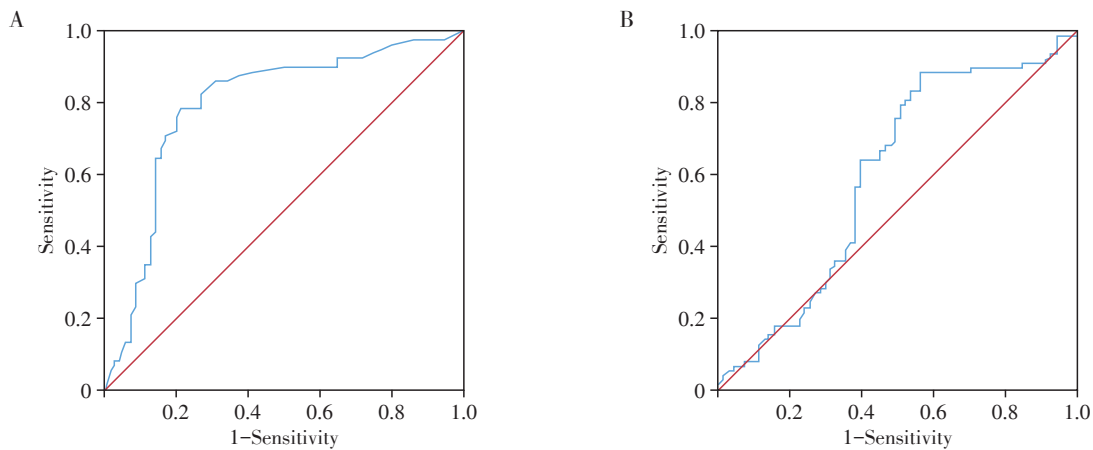
MTB是全世界最常见的肺肉芽肿病因,但一些组织病理学检测结果发现,肉芽肿和坏死也在其他许多疾病中发现,包括异物、结节病、真菌感染等^[23],此外,根据呼吸系统病理标本的检查及取材规范,肺组织活检和穿刺标本应全部取材,手术切除标本中,较小的病灶尽量完整切除;对于较大的病变,要从病变中心及边缘多部位取材,以全面反映病



The square of each line illustrates the OR value; the horizontal line indicates the confidence interval.

图4 组织病理学参数与qPCR结果相关性分析的森林图

Figure 4 Forest plot for the correlation analysis between histopathological parameters and qPCR results



A: The ROC curve of the percentage of necrotic area. B: The ROC curve of the maximum diameter of granulomas.

图5 坏死面积百分比和肉芽肿最大直径检测qPCR阳性结果的ROC曲线分析

Figure 5 ROC curve analysis of the diagnostic efficacy for positive qPCR result by the percentage of necrotic area and the maximum diameter of granulomas

变情况^[24],每一个病例需制作2~10个对应的甲醛固定、石蜡包埋标本。然而MTB在每个石蜡标本间、甚至同一个石蜡标本的不同切片间的分布并不均匀,因此,在每个病例的数张切片中初筛疑似TB感染的标本,针对性进行后续qPCR检测,对提高TB的诊断效率和准确性尤为重要。

既往研究显示,MTB分泌蛋白Ag85B在TB的干酪样坏死灶及周围分布更广,分子检测技术同样对肉芽肿中干酪样坏死组织的MTB遗传物质更敏感,即使菌量少或包裹在坏死组织中,也能通过扩增技术被检出^[25-26]。以上报道表明,肉芽肿伴随广泛的干酪样坏死是MTB富集区,选择特征性FFPE标本,或许可以提高检测的灵敏度。因此,本研究首先通过HE染色初筛149例具有典型TB肉芽肿性炎症特征的标本蜡块,进行Z-N抗酸染色和qPCR分子检测。

Z-N抗酸染色是重要的TB诊断工具,可快速提供结果,特别是对于微生物负荷高、传播风险大和需

要快速开始治疗的患者具有十分重要的意义^[27-28]。然而,本研究结果和既往研究报道一致^[29],Z-N抗酸染色的灵敏度(56.8%)和特异度(42.6%)有限。抗酸杆菌在染色标本中出现的概率与患者痰液中的杆菌数量呈正比,如果每毫升低于1 000个,发现抗酸杆菌的概率将低于10%^[30]。为提高这些测试的灵敏度,可能需要在几个临床标本上重复这些测试,导致资源、时间和人力的浪费。Z-N抗酸染色阳性标本在显微镜下很难区分MTB感染和非MTB感染,因为两者都耐酸且形态相似,这可能导致Z-N抗酸染色出现一定比例的假阳性结果,特异度降低。

qPCR分子检测在TB诊断中显示出更高的灵敏度、特异度和与临床诊断的一致性。世界卫生组织等认为PCR技术的出现,提高了TB的诊断率,具有检测限低(每毫升10~1 000个菌落形成单位),诊断时间短(2~6 h)等优点^[31-32]。qPCR可针对性检测仅存在于MTB中的插入元件IS6110靶基因,对TB检测的特异性强,能够筛选出Z-N抗酸染色不能区别

的染色阳性但非TB感染。本研究中2例石蜡组织Z-N抗酸染色阳性,而qPCR阴性,最终通过其他实验室试剂盒鉴定为NTM感染,1例为Chelonae分枝杆菌亚种,另1例为鸟分枝杆菌。虽然分子技术检测TB有效和直接,但成本较高^[33]。另有其他研究认为,qPCR的特异性强,但可能不够敏感,其可靠性受到一些组织学特征的影响^[34-35]。本研究中,在经HE染色筛选后具有典型病理特征的标本检测中,qPCR特异度较高,为96.3%,灵敏度也达到80.0%,高于既往qPCR技术在肉芽肿FFPE组织中灵敏度为26.3%~77.63%的报道^[36-38]。

本研究以此为切入点,将149例标本分为qPCR阳性组和阴性组,回顾性观察了两组HE染色结果,并总结了它们的组织病理学特征,分析qPCR灵敏度得以提高的具体原因,例如彻底干酪样坏死面积百分比(有核破裂碎片、无细胞的粉红色坏死区域面积 $\geq 25\%$,或坏死面积 $< 25\%$),每张切片的肉芽肿数量和大小(最大直径 ≥ 8 mm或最大直径 < 8 mm)、是否有融合性肉芽肿(合并肉芽肿的相邻边界)、是否有离散肉芽肿(界限清楚,大部分上皮样组织细胞符合肉芽肿的形状)、坏死外层是否伴有上皮样组织细胞聚集带、肉芽肿周围是否有淋巴细胞层、是否有朗汉斯巨细胞等。本研究结果表明:当标本的干酪样坏死面积百分比 $\geq 25\%$ ($\chi^2=41.649, P < 0.001$),肉芽肿最大直径 ≥ 8 mm($\chi^2=8.071, P=0.004$)时,更常提示为qPCR阳性。通过二元Logistic回归分析和ROC曲线分析AUC,这两个因素对qPCR阳性结果的诊断都具有较高的灵敏度,提示它们对qPCR检测TB可能有一定的辅助诊断价值。这可能是随着疾病进展而形成肉芽肿,MTB具有高活性和高复制能力,导致典型的干酪样坏死和肉芽肿形成,此时细菌代谢活跃且载量高,所以更容易通过qPCR检测到。但本研究没有观察到qPCR检测结果与两个因素之间的线性关系。此外,肉芽肿最大直径 ≥ 8 mm对TB的预测特异度(43.7%)低于干酪样坏死面积百分比 $\geq 25\%$ (78.9%),这提示其单独应用的参考价值有限,可能需结合干酪样坏死面积或坏死类型等指标进行综合判断。

由此可见,出于成本和时间效益考虑,可以广泛使用常规HE染色辅助TB诊断。HE染色对TB初筛的灵敏度高(149/189, 78.8%),特异度差(95/189, 50.3%)。但是,如果它与特异度高而灵敏度较差的qPCR检测一起使用,可以成为一个方便的诊断工具。选择HE染色中具有干酪样坏死面积百分比 \geq

25%和肉芽肿最大直径 ≥ 8 mm等病理特征的蜡块进行qPCR检测,能够弥补qPCR检测灵敏度低的缺点,且更具成本、时间效益。

基于以上观察结果,同样提示在临床操作中,新鲜手术标本的取材应尽可能保留坏死物质。若病灶异质性明显,则需多点取样,避免漏检;组织固定也需及时,离体组织需在30 min之内用10%中性甲醛固定,防止细胞内的溶酶体酶释放破坏MTB结构,如细胞壁破裂、DNA/RNA降解,影响后续检测。

本研究考察了FFPE组织HE染色的定量病理特征与MTB qPCR检测灵敏度之间的关系,能够有效指导临床工作中对疑似TB标本进行合理取材,以及通过HE染色初筛适合的标本进行qPCR检测,更为经济、可靠、迅速地诊断TB。本研究存在一定局限性,标本采集方法不同,灵敏度和特异度存在差异,需要进一步扩大样本量来验证本研究的结果。

利益冲突声明:

所有作者声明无利益冲突。

Conflict of Interests:

All of the authors have no conflict of interests to declare.

作者贡献声明:

沈丽华负责初稿撰写、数据整理。张倩倩负责方法学、数据整理。金晓燕负责软件分析、数据整理。胡慧娣、董燕负责软件分析。邹珏负责验证、监督、调查、数据整理、撰写与审阅初稿。

Author's Contributions:

SHEN Lihua was responsible for data collection and writing, including the original draft as well as review and editing. ZHANG Qianqian contributed to methodology and data curation. JIN Xiaoyan handled software analysis, and data collection. HU Huidi and DONG Yan contributed to software analysis. ZOU Jue was involved in conceptualization, data curation, validation, supervision, investigation, writing and reviewing the original draft.

[参考文献]

- [1] NATARAJAN A, BEENA P M, DEVNIKAR A V, et al. A systemic review on tuberculosis [J]. Indian J Tuberc, 2020, 67(3): 295-311
- [2] TRAJMAN A, CAMPBELL J R, KUNOR T, et al. Tuberculosis [J]. Lancet, 2025, 405(10481): 850-866
- [3] LONG Q, GUO L, JIANG W X, et al. Ending tuberculosis in China: health system challenges [J]. Lancet Public Health, 2021, 6(12): e948-e953
- [4] TEO A K J, SINGH S R, PREM K, et al. Duration and determinants of delayed tuberculosis diagnosis and treatment in high-burden countries: a mixed-methods systematic review and meta-analysis [J]. Respir Res, 2021, 22

- (1):251
- [5] GONG W P, WU X Q. Differential diagnosis of latent tuberculosis infection and active tuberculosis: a key to a successful tuberculosis control strategy[J]. *Front Microbiol*, 2021, 12: 745592
- [6] ZHOU L H, YONG Y, RAN X Q, et al. Diagnostic value of the Xpert MTB/RIF assay combined with endobronchial ultrasonography with a guide sheath for peripheral nodular pulmonary tuberculosis[J]. *BMC Infect Dis*, 2024, 24(1): 1017
- [7] KABIR S, PARASH M T H, EMRAN N A, et al. Diagnostic challenges and gene-Xpert utility in detecting *Mycobacterium tuberculosis* among suspected cases of Pulmonary tuberculosis[J]. *PLoS One*, 2021, 16(5): e0251858
- [8] SHARMA M, BROOR S, MAHESHWARI M, et al. Comparison of conventional diagnostic methods with molecular method for the diagnosis of pulmonary tuberculosis[J]. *Indian J Tuberc*, 2023, 70(2): 182-189
- [9] STELLMACHER F, KIRFEL J, KALSDORF B, et al. Molecular pathology of tuberculosis: status, methodology, and limits[J]. *Pathologe*, 2021, 42(1): 78-82
- [10] MEIRELES S I, CRUZ M V, IRFFI G P, et al. Incidence of mycobacteria in pulmonary granulomatous lesions[J]. *Clinics*, 2025, 80: 100564
- [11] XU F F, BIAN K Y, WANG S W, et al. B and T lymphocyte attenuator as a C-reactive protein and IgA associated auxiliary diagnostic marker for pulmonary tuberculosis: a case-control study[J]. *Ann Transl Med*, 2022, 10(24): 1370
- [12] MACLEAN E, KOHLI M, WEBER S F, et al. Advances in molecular diagnosis of tuberculosis[J]. *J Clin Microbiol*, 2020, 58(10): e01582-19
- [13] LIANG J Q, AN H R, ZHOU J, et al. Exploratory development of PCR-fluorescent probes in rapid detection of mutations associated with extensively drug-resistant tuberculosis[J]. *Eur J Clin Microbiol Infect Dis*, 2021, 40(9): 1851-1861
- [14] PERUMAL P, ABDULLATIF M B, GARLANT H N, et al. Validation of differentially expressed immune biomarkers in latent and active tuberculosis by real-time PCR[J]. *Front Immunol*, 2020, 11: 612564
- [15] BABAFEMI E O, CHERIAN B P, OUMA B, et al. Paediatric tuberculosis diagnosis using *Mycobacterium tuberculosis* real-time polymerase chain reaction assay: a systematic review and meta-analysis[J]. *Syst Rev*, 2021, 10(1): 278
- [16] AYALEW S, WEGAYEHU T, WONDALE B, et al. Detection of *Mycobacterium tuberculosis* complex in saliva by quantitative PCR: a potential alternative specimen for pulmonary tuberculosis diagnosis[J]. *Tuberculosis (Edinb)*, 2024, 148: 102554
- [17] JO Y S, PARK J H, LEE J K, et al. Discordance between MTB/RIF and real-time tuberculosis-specific polymerase chain reaction assay in bronchial washing specimen and its clinical implications[J]. *PLoS One*, 2016, 11(10): e0164923
- [18] JIANG F M, HUANG W W, WANG Y, et al. Nucleic acid amplification testing and sequencing combined with acid-fast staining in needle biopsy lung tissues for the diagnosis of smear-negative pulmonary tuberculosis[J]. *PLoS One*, 2016, 11(12): e0167342
- [19] ADDO S O, ABRAHAMS A O D, MENSAH G I, et al. Utility of anti-*Mycobacterium tuberculosis* antibody (ab905) for detection of mycobacterial antigens in formalin-fixed paraffin-embedded tissues from clinically and histologically suggestive extrapulmonary tuberculosis cases[J]. *Heliyon*, 2022, 8(12): e12370
- [20] STELLMACHER F, PERNER S. Histopathology of pulmonary tuberculosis[J]. *Pathologe*, 2021, 42(1): 71-77
- [21] NIYONKURU A, CHEN X M, BAKARI K H, et al. Evaluation of the diagnostic efficacy of ¹⁸F-fluorine-2-deoxy-D-glucose PET/CT for lung cancer and pulmonary tuberculosis in a tuberculosis-endemic country[J]. *Cancer Med*, 2020, 9(3): 931-942
- [22] HUANG M L, MA Y, JI X Y, et al. A study of risk factors for tuberculous meningitis among patients with tuberculosis in China: an analysis of data between 2012 and 2019[J]. *Front Public Health*, 2023, 10: 1040071
- [23] ROSEN Y. Pathology of granulomatous pulmonary diseases[J]. *Arch Pathol Lab Med*, 2022, 146(2): 233-251
- [24] 陈杰. 病理标本的检查及取材规范[M]. 北京: 中国协和医科大学出版社, 2013: 20-40
- CHEN J. Examination and sampling standards for pathological specimens[M]. Beijing: Peking Union Medical College Publishing House, 2013: 20-40
- [25] DONG Y J, ZHOU L J, ZHANG C, et al. Detection of antigen Ag85B expression is useful for the diagnosis of tuberculosis, especially for those with an antituberculosis treatment history[J]. *Am J Clin Pathol*, 2023, 160(1): 62-71
- [26] SUN J, ZHOU X C, YU J, et al. Diagnostic value of tuberculosis-specific antigens Ag85B, ESAT-6 and CFP10 in pulmonary tuberculosis[J]. *J Clin Tuberc Other Mycobact Dis*, 2024, 37: 100486
- [27] ARTETA A A, ARIAS L F, CADAVID C E. Ziehl-Neelsen stain in the pathology laboratory: performance and diagnostic aid for mycobacteria in bronchoalveolar lavage[J]. *Biomedica*, 2022, 42(3): 460-469
- [28] ZURAC S, MOGODICI C, PONCU T, et al. A new artificial intelligence-based method for identifying *Mycobacte-*

- rium tuberculosis* in Ziehl-Neelsen stain on tissue[J]. *Diagnosics*(Basel), 2022, 12(6): 1484
- [29] 李小燕, 吴丹, 姚梅宏, 等. 抗酸染色和即时荧光定量PCR法检测结核分枝杆菌在辅助诊断肺结核中的作用比较[J]. *中华病理学杂志*, 2018, 47(2): 132-134
- LI X Y, WU D, YAO M H, et al. Comparison of the role of acid-fast staining and real-time fluorescence quantitative PCR in the auxiliary diagnosis of pulmonary tuberculosis [J]. *Chinese Journal of Pathology*, 2018, 47(2): 132-134
- [30] ANTONELLO M, SCUTARI R, LAURICELLA C, et al. Rapid detection and quantification of *Mycobacterium tuberculosis* DNA in paraffinized samples by droplet digital PCR: a preliminary study[J]. *Front Microbiol*, 2021, 12: 727774
- [31] MOURE Z, CASTELLVÍ J, SÁNCHEZ-MONTALVÁ A, et al. The role of molecular techniques for the detection of *Mycobacterium tuberculosis* complex in paraffin-embedded biopsies [J]. *Appl Immunohistochem Mol Morphol*, 2019, 27(1): 77-80
- [32] OPOTA O, ZAKHAM F, MAZZA-STALDER J, et al. Added value of Xpert MTB/RIF ultra for diagnosis of pulmonary tuberculosis in a low-prevalence setting [J]. *J Clin Microbiol*, 2019, 57(2): e01717-18
- [33] NOUR NEAMATOLLAHI A, TARASHI S, EBRAHIMZADEH N, et al. Evaluation of miR-let-7f, miR-125a, and miR-125b expression levels in sputum and serum samples of Iranians and Afghans with pulmonary tuberculosis [J]. *Iran J Microbiol*, 2023, 15(5): 665-673
- [34] KIM Y N, KIM K M, CHOI H N, et al. Clinical usefulness of PCR for differential diagnosis of tuberculosis and non-tuberculous mycobacterial infection in paraffin-embedded lung tissues [J]. *J Mol Diagn*, 2015, 17(5): 597-604
- [35] URER H N, GUNLUOGLU M Z, UNVER N, et al. Benign solitary pulmonary necrotic nodules: how effectively does pathological examination explain the cause? [J]. *Can Respir J*, 2020, 2020: 7850750
- [36] HASHMI A A, NAZ S, YAQEEEN S R, et al. Utility of the GeneXpert *Mycobacterium tuberculosis*/rifampin (MTB/RIF) assay on paraffin-embedded biopsy tissue samples for detecting tuberculosis: comparison with histopathology [J]. *Cureus*, 2020, 12(12): e12048
- [37] LIU Q B, XU F, LIU Q L, et al. Comparative analysis of five etiological detecting techniques for the positive rates in the diagnosis of tuberculous granuloma [J]. *J Clin Tuberc Other Mycobact Dis*, 2023, 32: 100378
- [38] PANDEY S, CONGDON J, MCINNES B, et al. Evaluation of the GeneXpert MTB/RIF assay on extrapulmonary and respiratory samples other than sputum: a low burden country experience [J]. *Pathology*, 2017, 49(1): 70-74
- [收稿日期] 2025-02-26
(本文编辑: 陈汐敏)



欢迎关注本刊微博、微信公众号!